Brazilian Journal of Physics
ISSN: 0103-9733
luizno.bjp@gmail.com
Sociedade Brasileira de Física
Brasil

Rodríguez-Pérez, Sergio; Novaes, Marcel

Influence of a Superconducting Lead on Orbital Entanglement Production in Chaotic Cavities

Brazilian Journal of Physics, vol. 45, núm. 5, 2015, pp. 532-537
Sociedade Brasileira de Física
São Paulo, Brasil

Braz J Phys (2015) 45:532–537
DOI 10.1007/s13538-015-0348-5

CONDENSED MATTER

Influence of a Superconducting Lead on Orbital Entanglement Production in Chaotic Cavities

Sergio Rodríguez-Pérez[1] · Marcel Novaes[2]

Received: 3 June 2015 / Published online: 25 July 2015

Abstract We study orbital entanglement production in a chaotic cavity connected to four single-channel normal-metal leads and one superconducting lead, assuming the presence of time-reversal symmetry and within a random matrix theory approach. The scattered state of two incident electrons is written as the superposition of several two-outgoing quasi-particle components, four of which are orbitally entangled in a left-right bipartition. We calculate numerically the mean value of the squared norm of each entangled component, as functions of the number of channels in the superconducting lead. Its behavior is explained as resulting from the proximity effect. We also study statistically the amount of entanglement carried by each pair of outgoing quasi-particles. When the influence of the superconductor is more intense, the device works as an entangler of electron-hole pairs, and the average entanglement is found to be considerably larger than that obtained without the superconducting lead.

Keywords Orbital entanglement · Chaotic cavity · Superconductor

✉ Sergio Rodríguez-Pérez
sergio.rodriguez@ect.ufrn.br

[1] Escola de Ciências e Tecnologia, Universidade Federal do Rio Grande do Norte, Natal, RN, 59072-970, Brazil

[2] Instituto de Física, Universidade Federal de Uberlândia, Uberlândia, MG, 38400-902, Brazil

1 Introduction

Quantum correlations are at the very heart of quantum physics [1] and of applications like quantum computing and quantum cryptography [2]. The ability of quantum transport devices to produce and manipulate entanglement has been explored during the last years [3–16]. Several of those devices produce orbital entanglement from scattering processes taking place inside one of its parts. In a seminal work [5], it was proposed to use a chaotic cavity as quantum entangler. The system consists of a cavity ideally connected to four one-channel normal-metal leads, two at the left and two at the right. An electron leaving the cavity at either the left or the right represents a qubit, and entanglement between two qubits can be studied considering a left-right bipartition.

The mean value and the variance of the concurrence, a quantifier of entanglement, were initially calculated using random matrix theory [5], followed by more complete statistical analysis [6]. Non-ideal contacts [7, 8] and spin-orbit interaction [9] have also been considered. Constraints on entanglement production imposed by the geometry of the device were explored [10], and it was found that more entangled states are less likely to be produced in general. Recently, a quantum wire [11] and a Dirac billiard [12] were also used as quantum entanglers.

Many normal-superconducting (NS) hybrid systems have also been proposed as a source of entanglement [13–16]. Entangled pairs of quasi-particles can be generated after Andreev reflections which take place at the normal-superconductor interface. In the present work, we propose the use of a chaotic cavity connected to a superconducting lead as orbital entangler. Within random matrix theory, we study the generation probability of each pair of entangled quasi-particles, and how this quantity and the amount of entanglement are affected by the proximity effect. As the influence of the superconductor is more intense, the probability of producing one left-outgoing hole and one right-outgoing electron is found to dominate over those characterizing other entangled pairs, in the presence of time-reversal symmetry. There is also a notable increase in the production of entanglement, induced by the proximity effect [17], when compared to normal cavities.

The paper is organized as follows. In Section 2, we explain how the device is designed, and what is the structure of its scattering matrix. We also write the scattered state as a function of the transmission properties of the system. The mean value of the squared norms of entangled states is analyzed in Section 3. Statistics of concurrence is studied in Section 4. We present its full distribution, as well as its mean value and variance, for different values of the number of open channels in the superconducting lead. We summarize and conclude in Section 5. An additional section, Appendix A is included to explain how to calculate the scattering matrix of the system.

2 Design of the Device

The setup is represented in Fig. 1. A central chaotic cavity is connected to five leads. Four leads are normal and have only one open conduction channel; they are represented at the left and right sides of the cavity and denoted by L_1, L_2, R_1, and R_2. A superconducting lead with N_s channels is attached to the top of the cavity. A potential V is applied on the left leads and the right ones are grounded. The superconducting lead is grounded. Thus, an electrical current crosses the device. Specifically, pairs of electrons with energies between the Fermi energy E_F and $E_F + eV$ enter the cavity from the left leads. It is assumed that the energy of the incident electrons is much smaller than the gap Δ in the superconductor, $eV \ll \Delta$. This implies that charge transfer in the NS interface takes place only via Andreev reflection [18]. One quasi-particle leaving the cavity by the left/right leads represents a qubit. Since the device has only one superconducting lead, the phase of the superconductor is irrelevant. We also neglect temperature fluctuations.

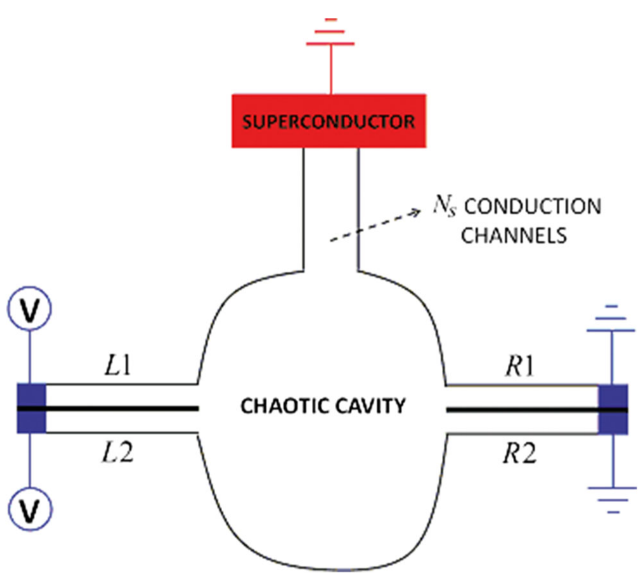

Fig. 1 (Color online) A chaotic cavity is attached to four normal leads, denoted by L_1, L_2, R_1 and R_2, and one grounded superconducting lead. Each normal lead has one conduction channel while there are N_s open channels in the superconducting lead. A potential V is applied on the left leads and the right leads are grounded

2.1 Scattering Matrix

The potential V is small enough to neglect the dependence on energy of the scattering matrix of the system, which is denoted by S_{NS} and has the following left-right structure:

$$S_{NS} = \begin{pmatrix} \hat{r} & \hat{t}' \\ \hat{t} & \hat{r}' \end{pmatrix}. \tag{1}$$

The blocks $\hat{r}$ ($\hat{r}'$) and $\hat{t}$ ($\hat{t}'$) contain, respectively, the reflection and the transmission amplitudes for quasi-particles coming from the left (right). Each block has its own electron-hole structure, which is indicated with the hat symbol. For example, the matrix $\hat{r}$ is

$$\hat{r} = \begin{pmatrix} r^{ee} & r^{eh} \\ r^{he} & r^{hh} \end{pmatrix}. \tag{2}$$

Moreover, each sub-block $r^{\alpha\beta}$ in the last equation is a 2×2 matrix, whose elements are the reflection amplitudes for the leads L_1 and L_2. They are given by

$$r^{\alpha\beta} = \begin{pmatrix} r_{11}^{\alpha\beta} & r_{12}^{\alpha\beta} \\ r_{21}^{\alpha\beta} & r_{22}^{\alpha\beta} \end{pmatrix}. \tag{3}$$

This is the channel structure. The other blocks have similar structures.

The scattering matrix S_{NS} carries the transmission properties of all the parts of the model. In particular, it contains the scattering properties of the cavity, and the interface between the cavity and the superconducting lead. How to define the scattering matrix of each part of the system and make their composition to obtain S_{NS} is explained in Appendix A.

Due to the underlying chaotic dynamic in the cavity, the statistical properties of transport are universal and well described by random matrix theory. Thus, the quality of randomness is incorporated into S_{NS} through the scattering matrix of the cavity, which is a unitary symmetric matrix and can be taken as uniformly distributed in the so-called Circular Orthogonal Ensemble. This ensemble is appropriate to model chaotic cavities ideally connected to normal leads, in the presence of time-reversal symmetry and spinless particles [19]. In our numerical simulations, we generate these matrices using an algorithm of Mezzadri [20].

2.2 Scattered State

The scattered state of two incident electrons can be expressed as $|\Psi_{\rm scat}\rangle = |\Psi_{LL}\rangle + |\Psi_{RR}\rangle + |\Psi_{LR}\rangle$. State $|\Psi_{LL}\rangle$ ($|\Psi_{RR}\rangle$) characterizes two quasi-particles being scattered to the left (right). One quasi-particle scattered to the left and the other one to the right is represented by the state $|\Psi_{LR}\rangle$. There are two forms of entanglement, the so-called occupation-number and orbital entanglement, which are related to the scattered state. All the three components contribute to the occupation-number entanglement, while only the left-right component is responsible for the orbital entanglement [21]. As we are interested in the latter, we will focus on $|\Psi_{LR}\rangle$.

In order to give an explicit expression for this state, we define the projector matrix

$$\sigma' = \mathrm{i}\,\sigma_y \otimes \begin{pmatrix} 1 & 0 \\ 0 & 0 \end{pmatrix}, \qquad (4)$$

where σ_y is one of the Pauli matrices defined in the channel space, and the second matrix in the right hand side is a projector on the electron-hole space. The structure of σ' accounts for the fact that the incident state is given by two electrons coming from the left. It is also convenient to define the fermionic operators $\mathcal{L}_j^{\alpha}$ and $\mathcal{R}_j^{\alpha}$, which create a quasi-particle of type α going out at the lead L_j and R_j, respectively, with energy ϵ if $\alpha = e$ and $-\epsilon$ if $\alpha = h$ ($E_F < \epsilon < E_F + eV$). We also define

$$\hat{\gamma} = \hat{r}\sigma'\hat{t}^{T}, \qquad (5)$$

where $\hat{t}^{T}$ is the transpose of $\hat{t}$. Using the above objects, the left-right states can be expressed in the following way:

$$|\Psi_{LR}\rangle = \sum_{jk;\alpha\beta} \gamma_{jk}^{\alpha\beta}\ \mathcal{L}_j^{\alpha}\ \mathcal{R}_k^{\beta}\ |0\rangle. \qquad (6)$$

In the last equation, $|0\rangle$ is the state without electronic excitations. If the sum over j and k is performed, it leads to the superposition $|\Psi_{LR}\rangle = \sum_{\alpha\beta} |\Psi^{\alpha\beta}\rangle$, where $|\Psi^{\alpha\beta}\rangle$ represents the quasi-particle α getting out at the left, and β getting out at the right.

3 Statistics of the Squared Norms

In this section, we focus on the probability of producing, during a fixed time, a given number of entangled pairs α and β. This probability is determined by the squared norm of the state $|\Psi^{\alpha\beta}\rangle$, namely, $\mathcal{N}^{\alpha\beta} = \langle\Psi^{\alpha\beta}|\Psi^{\alpha\beta}\rangle$. Using Eq. 6, it can be expressed as a function of the transmission properties of the system through the following equation:

$$\mathcal{N}^{\alpha\beta} = \mathrm{Tr}(\gamma^{\alpha\beta\dagger}\gamma^{\alpha\beta}). \qquad (7)$$

Let us discuss the underlying mechanism behind the influence of proximity effects on transport properties. As the number of open channels in the superconducting lead increases, the probability of incident electrons to undergo an Andreev reflection in the NS interface and thus to be backscattered as holes to the left before "feeling" the chaos of the cavity gets larger. As $N_s \to \infty$, this probability becomes unit, and the device works as if all electrons were Andreev reflected upon arrival at the cavity [22].

A consequence of *direct Andreev backscattering* is an increased number of holes leaving the cavity at the left, and therefore a decreased transmission of any quasi-particle to the right. This is verified in Fig. 2, where we present the average value of square norms as functions of N_s. As N_s grows, $\overline{\mathcal{N}}^{ee}$ and $\overline{\mathcal{N}}^{eh}$ monotonically decrease, because the probability of an electron to be scattered to the left continually decreases. On the other hand, $\overline{\mathcal{N}}^{he}$ and $\overline{\mathcal{N}}^{hh}$ have a non-monotonic behavior, initially increasing due to direct Andreev backscattering. The quantity $\overline{\mathcal{N}}^{he}$ decreases more slowly than the other squared norms, which suggests that scattering to the right is more probable for electrons than for holes.

The dominance of $\overline{\mathcal{N}}^{he}$ over the other entangled components can be quantified by

$$E_r = \frac{\overline{\mathcal{N}}^{ee} + \overline{\mathcal{N}}^{eh} + \overline{\mathcal{N}}^{hh}}{\overline{\mathcal{N}}^{he}}. \qquad (8)$$

The behavior of E_r is shown in Fig. 3, where N_s runs from 25 to 400. The decay follows a power law with exponent approximately equal to -1. Notice that for $N_s = 400$, the

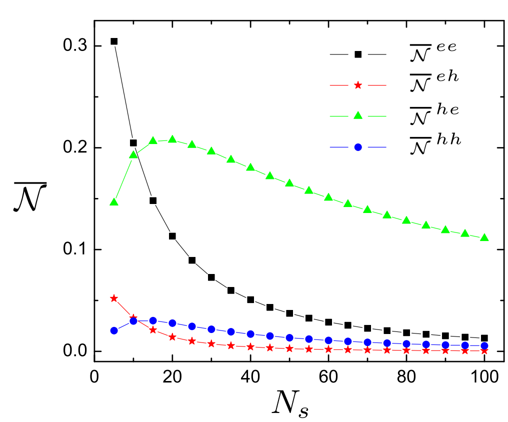

Fig. 2 (Color online) Mean values of the squared norms $\mathcal{N}^{\alpha\beta}$ are represented for different numbers of open channels in the superconducting lead. 10^5 samples were generated for each value of N_s

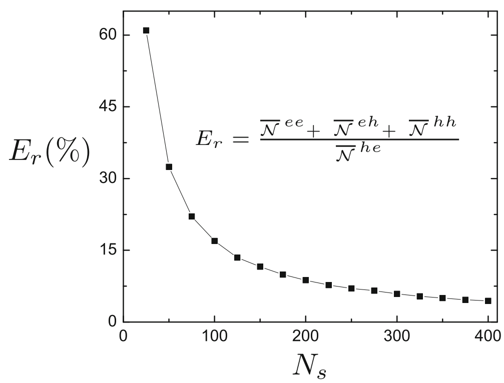

Fig. 3 Function E_r (in percent) for values of N_s varying from 25 to 400. Each dot was calculated using 5×10^3 random matrices

sum of the other components represents less than 5 % of $\overline{\mathcal{N}}^{he}$. This means that for very large values of N_s, entanglement is almost entirely carried by pairs of left-outgoing holes and right-outgoing electrons.

Direct Andreev backscattering does not occur if TRS is broken, because a random phase is accumulated during the process and so it is killed after averaging. An implication of this is that in the presence of a magnetic field and for $N_s \gg 1$, the statistical distributions of $\mathcal{N}^{\alpha\beta}$ are very similar for any α and β. We corroborated this observation through numerical simulations (not shown).

4 Statistics of Concurrence

The concurrence that characterizes the state $|\Psi^{\alpha\beta}\rangle$ is given by [23, 24]

$$\mathcal{C}^{\alpha\beta} = 2\sqrt{\mathrm{Det}(\gamma^{\alpha\beta}\gamma^{\alpha\beta\dagger})}/\mathrm{Tr}(\gamma^{\alpha\beta}\gamma^{\alpha\beta\dagger}). \tag{9}$$

In contrast with the result obtained for a generic normal system [5], this expression depends not only on the eigenvalues of the normal scattering matrix, but on its eigenvectors as well.

Figure 4 shows the distributions of concurrence for $N_s =$ 5, 25, and 100. They suggest that all pairs of left-right outgoing quasi-particles are entangled, but none of them is maximally entangled. It is clearly seen that $\mathcal{C}^{he}$ is the quantity most sensitive to the presence of the superconductor. However, variations are small for all the distributions when N_s is large, which indicates convergence, as can be observed in Fig. 5 where we show the average value and the variance of the concurrence.

As the number N_s increases, there is a remarkable enhancement in the production of entanglement for the hole-electron component: $\overline{\mathcal{C}}^{he}$ reaches values above 0.58, reflecting a considerable increase compared to the normal case, where $\overline{\mathcal{C}} \approx 0.38$ [5]. Note that the other three components have only slight dependence on N_s. Moreover, variations of $\mathcal{C}^{he}$ from sample to sample are more concentrated around its mean value than for the other components. The variance of this quantity decreases as N_s increases (see Fig. 5b). We found that var($\mathcal{C}^{he}$) oscillates around 0.053 for large N_s. This value is slightly less than the variance for the other components, as well as those found for a normal cavity [5].

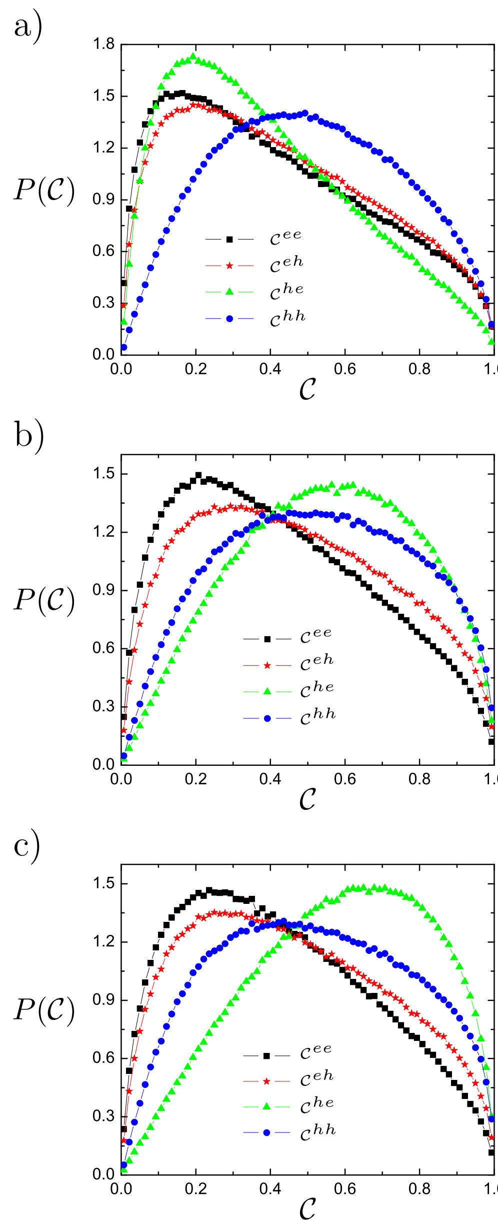

Fig. 4 (Color online) Distributions of concurrence are represented for N_s equal to **a** 5, **b** 25, and **c** 100. Each distribution was made using 10^6 random matrices

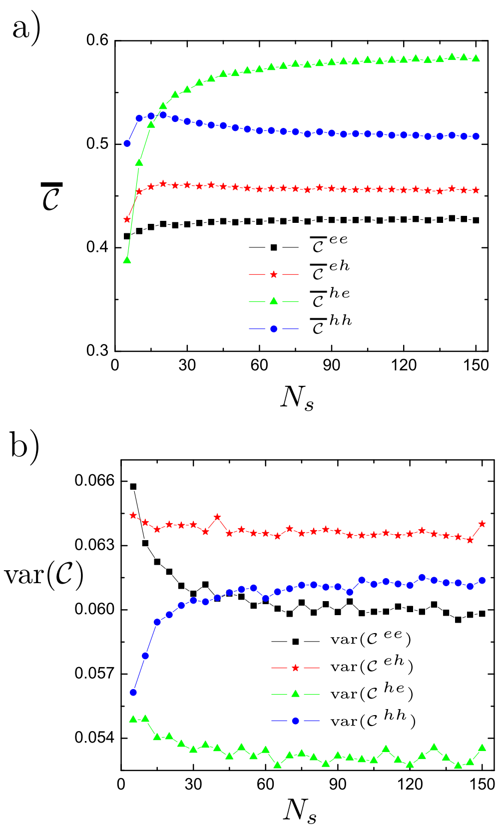

Fig. 5 (Color online) **a** Mean value and **b** variance of the concurrence calculated from 10^5 random matrices for each value of N_s

5 Conclusion

We studied orbital entanglement production in a chaotic cavity connected to a superconducting lead, assuming time-reversal symmetry in the system. Numerical simulations were performed to statistically analyze the squared norm and the concurrence of states describing an entangled pair of outgoing quasi-particles. The behavior of the squared norm for varying numbers of channels in the superconducting lead was explained as a consequence of Andreev reflection. Even though the norms of the entangled components decrease as the influence of the superconductor is stronger, the squared norm of the state describing one left-outgoing hole and one right-outgoing electron dominates, and thus the device behaves as an entangler of electron-hole pairs. In this regime, there is a notable enhance in the amount of entanglement for that state, exceeding the value found for a normal cavity.

Acknowledgments This work was partially supported by grant 2011/07362-0, São Paulo Research Foundation (FAPESP).

Appendix A: Calculation of the Scattering Matrix of the System

In this appendix, we explain how to calculate the scattering matrix S_{NS} after generating the random matrix that describes the cavity, which will be denoted by S_0. It will be divided in blocks, in the following way:

$$S_0 = \begin{pmatrix} r_0 & t'_0 \\ t_0 & r'_0 \end{pmatrix}. \tag{10}$$

Each block has dimensions $N_s \times N_s$, thus S_0 mixes $2N_s$ channels.

On the one hand, the interface between the cavity and the superconducting lead is characterized by N_s conduction channels. On the other hand, there are 4 open channels in the interface between the cavity and the normal leads. Therefore, we need to close the remaining $N_s - 4$ channels (it is assumed that $N_s > 4$). This is done introducing a fictitious barrier, which has a transparency very small (high) for $N_s - 4$ (four) channels. The scattering matrix that carries the information of the barrier can be written as

$$S_c = \begin{pmatrix} r_c & t'_c \\ t_c & r'_c \end{pmatrix}, \tag{11}$$

where all its blocks have dimensions $N_s \times N_s$. We also choose $r_c = r'_c$, $t_c = t'_c$, and define

$$r_c = \begin{pmatrix} \sqrt{\Gamma} I_4 & 0 \\ 0 & \sqrt{1-\Gamma} I_{N_s-4} \end{pmatrix}, \tag{12}$$

and

$$t_c = \mathrm{i} \begin{pmatrix} \sqrt{1-\Gamma} I_4 & 0 \\ 0 & \sqrt{\Gamma} I_{N_s-4} \end{pmatrix}, \tag{13}$$

Γ being the transparency of the barrier, a number much less than 1, and I_n the $n \times n$ identity matrix.

The interface between the cavity and the superconducting lead is described by a reflection matrix that encodes Andreev reflections. As the phase of the superconductor can be set equal to zero and the energy dependence is neglected, the reflection matrix can be written in the electron-hole space as [19]

$$r_A = -\mathrm{i} \begin{pmatrix} 0 & I_{N_s} \\ I_{N_s} & 0 \end{pmatrix}. \tag{14}$$

The factor $-\mathrm{i}$ in the last expression comes from the fact that quasi-particles gain a phase of $-\pi/2$ in each Andreev reflection.

First, it is necessary to compose S_0 and S_c, to obtain the total normal scattering matrix S_N. This is done using the following equations:

$$r_N = r_c + t_c M_N r_0 t_c, \quad (15)$$
$$t_N = \mathrm{i}\, t_0 (I_{N_s} + r_c M_N r_0) t_c, \quad (16)$$
$$r'_N = -r'_0 - t_0 r_c M_N t'_0, \quad (17)$$
$$t'_N = \mathrm{i}\, t_c M_N t'_0, \quad (18)$$

where $M_N = (I_{N_s} - r_0 r_c)^{-1}$.

Finally, using Eqs. 14–18, the blocks of S_{NS} in the electron-hole space can be written as [19]

$$S_{NS}^{ee} = r_N - t'_N (r'_N)^* M_e t_N, \quad (19)$$
$$S_{NS}^{hh} = r_N^* - (t'_N)^* r'_N M_h t_N^*, \quad (20)$$
$$S_{NS}^{eh} = -\mathrm{i}\, t'_N M_h t_N^*, \quad (21)$$
$$S_{NS}^{he} = -\mathrm{i}\, (t'_N)^* M_e t_N, \quad (22)$$

where $M_e = (I_{N_s} + r'_N (r'_N)^*)^{-1}$ and $M_h = M_e^*$.

S_{NS}^{eh} and S_{NS}^{hh} are not necessary to calculate norm and concurrence, because we consider the initial state given by two electrons entering the cavity from the left.

References

1. A. Einstein, B. Podolsky, N. Rosen, Phys. Rev. **47**, 777 (1935)
2. M.A. Nielsen, I.L. Chuang, *Quantum Computation and Quantum Information* (Cambridge University Press, Cambridge, 2000)
3. C.W.J. Beenakker, Proc. Int. School Phys. E Fermi **162** (2006)
4. Yu.V. Nazarov, Ya.M. Blanter, *Quantum Transport* (Cambridge University Press, Cambridge, 2009)
5. C.W.J. Beenakker, M. Kindermann, C.M. Marcus, A. Yacoby, Fundamental Problems of Mesoscopic Physics, in *NATO Science Series II,* vol. 154, ed. by I.V. Lerner, B.L. Altshuler, Y. Gefen (Kluwer, Dordrecht, 2004)
6. V.A. Gopar, D. Frustaglia, Phys. Rev. B **77**, 153403 (2008)
7. F.A.G. Almeida, A.M.C. Souza, Phys. Rev. B **82**, 115422 (2010)
8. D. Villamaina, P. Vivo, Phys. Rev. B **88**, 041301(R) (2013)
9. D. Frustaglia, S. Montangero, R. Fazio, Phys. Rev. B **74**, 165326 (2006)
10. S. Rodríguez-Pérez, M. Novaes, Phys. Rev. B **85**, 205414 (2012)
11. A. Aleta, H. Villarrubia-Rojo, D. Frustaglia, V.A. Gopar, Phys. Rev. B **89**, 075429 (2014)
12. J.G.G.S. Ramos, I.M.L. da Silva, A.L.R. Barbosa, Phys. Rev. B **90**, 245107 (2014)
13. G.B. Lesovik, T. Martin, G. Blatter, Eur. Phys. J. B **24**, 287 (2001)
14. P. Samuelsson, E.V. Sukhorukov, M. Büttiker, Phys. Rev. Lett. **91**, 157002 (2003)
15. Z.Y. Zeng, L. Zhou, J. Hong, B. Li, Phys. Rev. B **74**, 085312 (2006)
16. S. Franceschi, L. Kouwenhoven, C. Schönenberger, W. Wernsdorfer, Nat. Nano **5**, 703 (2010)
17. W.L. McMillan, Phys. Rev. Lett. **175**, 537 (1968)
18. A.F. Andreev, Zh. Eksp. Teor. Fiz **46**, 1823 (1964) [Sov. Phys. JETP **19**, 1228 (1964)]
19. C.W.J. Beenaker, Rev. Mod. Phys. **69**, 731 (1997)
20. F. Mezzadri. arXiv: math-ph/0609050v2 (2007)
21. V. Giovannetti, D. Frustaglia, F. Taddei, R. Fazio, Phys. Rev. B **75**, 241305 (2007)
22. A.A. Clerk, P.W. Brouwer, V. Ambegaokar, Phys. Rev. B **62**, 10226 (2000)
23. W.K. Wootters, Phys. Rev. Lett. **80**, 2245 (1998)
24. C.W.J. Beenakker, C. Emary, M. Kindermann, J.L. van Velsen, Phys. Rev. Lett. **91**, 147901 (2003)